CHAPTER VII

SYNTHESIS AND CHARACTERIZATION OF INCLUSION COMPLEX OF DL-AMINOGLUTETHIMIDE WITH β-CYCLODEXTRIN AND ITS INNOVATIVE APPLICATION IN BIOLOGICAL SYSTEM: COMPUTATIONAL AND EXPERIMENTAL INVESTIGATIONS

Abstract: Our present study intended to investigate the encapsulation of DL-AGT within the lipophilic cavity of β-CD molecule. The consequential inclusion system was characterized by UV-Visible spectroscopy, ^{1}HNMR study, PXRD study, SEM study, FT-IR study. Molecular docking was performed for the inclusion complex to discover the most proper orientation and it was seen that the drug DL-AGT fits into the cavity of β-CD in 1:1 ratio which was also confirmed from the Job's plot. Furthermore, a comparison was done on the basis of cell viability between the drug and its inclusion complex.

Keywords: DL-AGT, β-CD, Molecular docking, 1:1 ratio, Cell viability

1. Introduction:

The drug DL-Aminoglutethimide, (±)-3-(4-aminophenyl)-3-ethylpiperidine-2,6-dione (DL-AGT), used as an aromatase inhibitor for the treatment of advanced breast cancer and Cushing's syndrome was preferred as a suitable molecule for this work. According to Biopharmaceutics Classication System, it is a class ll drug with low water solubility but have good permeability[1]. DL-Aminoglutethimide, the drug that we have dealt with can cause aromatase inhibition. It was initially introduced as an anticonvulsant but due to its side effects of acting as a potent inhibitor of several enzymes on adrenal cortex, it is no longer been used. These drawbacks of this drug twisted into a clinical advantage in the treatment of cushing syndrome and advanced breast cancer. The growth of certain tumors rest on specific hormones and that makes the basis of endrocrine therapy of breast cancer. DL-AGT is found to be effective in hormone dependent breast carcinoma by suppressing the estrogen level in post menopausal women. It hinders the conversion of androgen to estrogen.[2] Moreover, this drug is very effective in painful bone metastates. However Aminoglutethimide has its side effects because of its toxicity[3] such as lethargy, depression and rash besides its benefits[4].

Nowadays, molecular encapsulation is an important aspect to increase the bioavailability of certain drugs to retain their therapeutic activity. Potent drug delivery systems including biocompatible polymers, nanoparticles have already been explored. Cyclodextrin based drug delivery systems are found to be most effective and reliable due to their non-toxicity and biodegradability[5, 6]. Cyclodextrins or cycloamyloses are truncated cone shaped cavity polymer having a minimum number of 6-D(+) glucopyranose units linked by α-1,4 bonds[7]. They can be natural or semi-synthetic (oligosaccharides)[8]. The α, β and γ cyclodextrins and their derivatives are immensely used in pharmaceutical science. For parental drug delivery, oral administration, cyclodextrins are extensively used. The applications of CDs are even more than the above as they are able to make inclusion complexes with some specific molecules which will be fitted in the cavity. So the size of the entering guest molecule is also an important parameter here[9]**.** The interaction between the host and the guest molecules are mainly non-covalent e.g. ion-dipole, hydrogen bonding and van der Waals types. The most widely accepted host for complex formation is β-CD for its suitable cavity diameter and low production cost[10, 11]. β-cyclodextrin consists of seven α-D-glucopyranose unit joined by α-1,4 linkage[12]. Cyclodextrins are able to modify the pharmacological properties of the encapsulated active substances like solubility, bioavailability, chemical stability, dispersibility and toxicity so by preparing the inclusion complexes with cyclodextrin molecules it can be possible to enhance or improve such properties of the active compounds[13-16].

In our present work, encapsulation of DL-Aminoglutethimide within the nano cavity of β– cyclodextrin was established by UV-Vis study, IR spectroscopic study, Powder X-Ray Diffraction study, ^{1}H NMR study, 2D ROESY study, Scanning Electron Microscopic study. Job plot implies the stoichiometry of the complex as 1:1, UV-visible study has given a proper explanation of the thermodynamic parameters of the inclusion process and association constant of the complex. Furthermore, the in vitro cell viability study between the drug and the inclusion complex showed that the Inclusion complex is less toxic on human normal kidney cell line than the drug. By the process of inclusion we are aiming towards the improvement of the properties of the drug (DL-AGT) i.e. to increase its solubility as it has low solubility, enhance specificity and reduce toxicity. Most notably, the stability constant for the complexation of DL-AGT and β-CD by UV-visible

spectroscopy was already there in the literature, though the whole project was on TM-β-CD and DL-AGT inclusion phenomenon [17].

2. Experimental Section:

2.1. Materials

The drug DL-AGT (purity>98%, Molecular weight= 232.28g/mol) was purchased from TCI chemicals India PVT. LTD, β-CD (purity≥97%; Molecular weight=1134.98 g/mol) was purchased from Sigma Aldrich Germany and all the reagents are used without further purification.

2.2. Methods

DL-Aminoglutemide and β-CD were weighed using Mettler Toledo AG-285 (uncertainty ±0.1mg) and their solutions were prepared in 15% acetonitrile solution (Acetonitrile-water mixture) at 298.15 K. Other solutions of required strengths were prepared by mass dilution.

Fourier transform infrared spectra (FTIR) were recorded on a PerkinElmer 8300 FT-IR spectrometer (PerkinElmer, Inc., Germany) using KBr disk procedure. Samples were prepared as thin KBr disks with minute amount of sample at room temperature. The range of scanning was kept at 4000−400 cm^{-1}. ^{1}H-NMR study was executed in DMSO-$d_6$medium using BRUKER AVANCE NEO 400 MHz (Bruker Inc., Germany) instrument where the solvent residual peak was taken as internal standard. UV-Visible Spectroscopy was performed in Agilent 8453 spectrophotometer (USA). PXRD data were obtained from Bruker D8 Advance (Germany), Cu Kα radiation source 45 kV, λ= 1.5406 A^0 with scanning range was from 5° to 80°.The scanning electron micrographs were determined by JEOL JSM-IT 100 scanning electron microscope model.

2.3. Molecular Docking: Molecular docking process was employed for the virtual screening of the small guest molecule (DL-AGT) and a host (β-CD) to find the geometry of the inclusion complex through PyRx software[18]. This software is written in the Python programming language with an intuitive user interface that run on all major operating

systems (Linux, Windows, and Mac OS)used to determine the binding parameters as well as binding geometry. It is a combination of several softwares such as AutoDockVina, AutoDock 4.2, Mayavi, Open Babel, etc. PyRx uses Vina and AutoDock 4.2 as docking softwares. The input files host, guest in the .pdb format were changed to .pdbqtfiles using inbuilt Autodock vina software. After preparing the files, they were exposed to docking by means of AutoDockVina. Before starting the docking calculation a grid box was prepared around the host molecule. This resulted in a binding site center of 8.3636, 24.4146, and 1.2278 for the X, Y, and Z axes, respectively.Grid box dimensions were set to be X, Y, and Z conformations equal to 25, 25, and 25, respectively. The grid space size was assigned perfectly, which allows selecting search space for the host to perform docking with the guest, normally, at the binding site. The interaction between DL-AGT and the respective β-CD was interpreted using the Lamarckian genetic algorithm (LGA). Once the calculations were ended, result of binding affinity ($KJ.mol^{-1}$) of the most stable conformation of the host with the guest was provided by the software in the table 4.

2.4. In-vitro cell viability study: The cell viability study of the drug and the synthesized complex was investigated by MTT assay. HEK-293 (Human normal kidney cell line) was cultured in 96 well micro titre plate at 37 ^{o}C, in presence of 5% carbon dioxide (CO_2) at a density of 5×10^3 cells/well in 100µl DMEM (Dulbecco's Modified Eagle Medium) Ham F-12 culture medium. After 24 hours of incubation, drugs (DL- AGT, β-CD.DL-AGT) were added in each well at different concentrations (50µM, 100µM, 150µM, 200µM, 250µM, 300µM, 350 µM,400µM,450µM,500µM) in triplicate. Then, the micro titre plate was incubated under the same experimental condition. Next day, after discarding the culture media from the treated plate 10µl (5mg/ml) of MTT powder [3-(4,5-dimethylthiazol-2-yl)-2,5-diphenyltetrazolium bromide] dissolved in 1X PBS was added in each well. Plate was again kept into incubator for 3 hours in the above mentioned condition. Finally, a formazan solubilizer i.e. Isopropanol was added to each well containing MTT solution and was shaken for about 10 minutes. At last, the absorbance was recorded by a micro titre plate reader (SPECTROstar^{Nano},Germany) at 620 nm[19]. The solutions of the concerned samples were prepared in DMSO.

2.5. Preparation method of inclusion complex:

By mixing β-CD and DL-ADT in the molar ratio of 1:1, the IC has been prepared. 1.0mmol of DL-AGT was dissolved in 25 mL of 15% acetonitrile and 1.0 mmol of β-CD in 25 mL of distilled water. Keeping the β-CD solution on a magnetic stirrer, the DL-AGT guest solution was added slowly and the mixture was allowed to stir for 36 hrs at constant temperature of 50^0C. The suspension thus obtained was filtered and dried in oven at 70^0C for 7 hrs. Ultimately the solid powder was procured and stored in a dessicator for future use.

3. Results and discussion:

3.1. Job plot: In order to determine the stoichiometry of the host-guest inclusion complex the continuous variation method or the Job's method is applied[20]. Here a set of solutions of the drug (DL-AGT) and β-CD was prepared by varying the mole fraction of DL-AGT from 0-1 and from the UV-Vis spectroscopy the absorbance of all the solutions are checked at the λ_{max} (238nm). By plotting ΔA*R against R, Job plot is generated, where ΔA is the difference in absorbance of the guest without and with β-CD and R= [DL-AGT]/[DL-AGT+β-CD]. The R_{max} value obtained from the Job plot is 0.5 (figure.1.a) which signifies a 1:1 complexation of the guest and host molecule[21].

3.2. Association constants and thermodynamic parameters: The association constants of DL-AGT and β-CD IC were calculated at three different temperatures by UV-Vis spectroscopy measuring the change in the molar extinction coefficient of the guest molecule when it enters into the hydrophobic cavity of β-CD from the hydrophilic environment. The absorbance changes of DL-AGT were studied by gradually increasing the concentration of β-CD. Benesi-Hildebrand equation is used for the determination of association constant[20].

$$\frac{1}{\Delta A} = \frac{1}{\Delta\varepsilon[AGT]}\frac{1}{Ka[CD]} + \frac{1}{\Delta\varepsilon[AGT]} \qquad \text{(Equation 1)}$$

Where [AGT] and [CD] are the concentrations of the guest molecule and the cyclodextrin molecule, Δε refers to the change in the molar extinction coefficient and ΔA is the change

in the absorbance of DL-AGT on addition of CD. From the double reciprocal plot of the Benesi-Hildebrand equation we have calculated the association constants at three different temperatures(293.15K,303.15K,313.15K) and the linearity of the plot suggests the 1:1 stoichiometry of the host and the guest molecule[22].

Furthermore, the important thermodynamic parameters are determined from the plot of logka Vs 1/T using equation 2.

$$2.303\log ka = -\frac{\Delta H^\circ}{RT} + \frac{\Delta S^\circ}{R} \qquad \text{(Equation 2)}$$

The spontaneity of the process i.e. the free energy change is measured by the following equation 3.

$$\Delta G^\circ = \Delta H^\circ - T\Delta S^\circ \qquad \text{(Equation 3)}$$

Where, the symbols have their usual significance. Now the values of thermodynamic parameters suggest that the process of inclusion is exothermic, spontaneous and entropy restricted. This restriction in entropy may be due to the molecular association between the guest and host molecules [23].

3.3. Solubility Study of DL-AGT.β-CD inclusion complex:

The ethanolic solubility between pure DL-AGT and DL-AGT.β-CD inclusion complex was evaluated using UV–visible spectroscopy. The UV–vis spectrum of DL-AGT.β-CD inclusion complex in different concentration using ethanolic solution was shown in Fig. 2. DL-AGT was sparingly soluble in water, therefore the experiment was modeled in ethanolic phase and the solubility of DL-AGT in ethanol was greatly enhanced when there occurs the formation of DL-AGT.β-CD inclusion complex. DL-AGT displayed absorption maximum peak (λ_{max}) at about 238 nm in the inclusion complex as shown in Fig. 2A and all the calculations were carried out using the λ_{max} value. The peak positions were independent of the concentrations of DL-AGT.β-CD but peak intensities were increasing upon increasing concentration. The plot of absorbance of DL-AGT.β-CD at 238 nm vs. the concentration of DL-AGT.β-CD, gives us a straight line as shown in Fig.2B. According to the Lambert–Beer law, the absorption coefficient of DL-AGT.β-CD in ethanolic solution was evaluated as 0.0907 L $g^{-1}cm^{-1}$. The UV spectra of DL-AGT.β-CD inclusion complex with saturated concentrations in ethanolic solution was shown in the Figure S5. The

absorbance value of saturated solution of DL-AGT.β-CD(inclusion complex) was found to be 1.59873 (Figure S5). The solubilities of pure DL-AGT and DL-AGT.β-CD in ethanol at 25°C were listed in the Table S5. So, it was cleared from the Table S5 that DL-AGT.β-CD inclusion complex has greater solubility with 17.62 $mg.mL^{-1}$ over pure DL-AGT with 7 $mg.mL^{-1}$. These results revealed that the water-soluble host β-CD played a crucial role to improve the solubility of DL-AGT remarkably by the formation of DL-AGT.β-CD inclusion complex. From the above we can also have a clear idea about the aqueous solubility of DL-AGT as there occurred an enhancement of solubility in ethanol after inclusion. [24] [25]

3.4. PXRD STUDY:

The diffractogram (Figure 3) of the DL-AGT.β-CD complex shows the disappearance of some of the pure DL-AGT spectral lines at the 2Θ values of 12.38, 15.09, 16.75, 17.95, 24.92 and the β-CD spectral lines at the 2Θ values of 4.63, 9.11 and 12.63 as shown in Table 2. Additionally, the appearance of new spectral lines of DL-AGT.β-CD complex at the 2Θ values of 17.85 and 18.50 are observed with less intense peaks. It is well known that the peak at 2θ = ∼20° in cyclodextrin based inclusion complexes is a feature of "channel-type" packaging in β-CD where only the head-to-head arrangement has been noticed. The disappearance of some peaks and the generation of new peaks with less intensity in the spectra of DL-AGT.β-CD inclusion complex suggest some sort of interactions between the guest and host molecules.

3.5. FT-IR Spectroscopy: The formation of inclusion complex can also be explained with the help of FT-IR spectroscopy. It is important to note that when the inclusion complex is formed, several characteristic peaks of the guest molecule might be shifted, reduced or disappeared. The stretching and bending vibrations of the three components viz, DL-AGT, β-CD and their IC are shown in Figure4.

In case of DL-AGT, the most important bands present in the IR spectrum are those related to the imide and amino functional groups. The N–H, C-H, C-O and C–N stretching modes give strong bands situated at 3500–3200, 2964, 1687 and 1202 cm^{-1}. The stretching at 3467 cm^{-1} and 3375 cm^{-1} may be due to the 1^0 and 2^0 amines respectively present in the drug molecule. The aromatic C=C stretching vibrations for DL-AGT were found at 1625, 1515, 1448 cm^{-1}. Bending vibrations of -NH and -NH2 appearing at 1625 display strong

bands in the IR spectrum. However, in β-CD, the O-H stretching vibration appeared at 3424 cm^{-1}. The C-H stretching frequency for β-CD appeared at 2921 cm^{-1}, and bending vibration of C-O-C in β-CD appeared at 1153 cm^{-1}. When, the inclusion complex is formed, a broad hump is observed at 3388 cm^{-1}. The characteristic peak for C=O was observed at 1687 cm^{-1} in case of DL-AGT which get slightly shifted at 1693 cm^{-1} in the IC. And the aromatic C=C stretching vibrations for DL-AGT in complex were shifted to 1632, 1515, 1454 cm^{-1} as well as the peak intensity got reduced to some extent. Thus from the above explanation and from Figure 4, it is noteworthy to say that most of the signals of β-CD and DL-AGT have been highly shifted with less peak intensity in the inclusion complex implying some non-bonding interactions of the guest and host in the inclusion complex.

3.6.1.^{1}HNMR study: For the prediction of the structure of the inclusion complex, ^{1}HNMR spectroscopy is a very convenient method. It delivers detailed information about the position of the H nuclei present in the structure of the concerned molecule/complex. As the host-guest inclusion process is based on weak non-bonding interactions, the changes occur in the chemical shifts values after inclusion are comparatively small than in other cases[26].

In β-CD, H3,H5 protons are located inside the cavity (H3 close to the wider rim and H5 close to the narrower rim) and H6 outside the cavity, near to the narrower rim[27]. When the guest molecule enters the cavity of β-CD, the protons inside the cavity (H3, H5) would definitely show some changes in chemical shift than that before[28]. It is observed that after inclusion H3 and H5 protons of β-CD were shifted to upfield but to a smaller extent.The ^{1}H-NMR spectra of DL-AGT, β-CD and inclusion complex were shown in Figure 5. Numerous peaks were found in the spectrum of DL-AGT as well as in β-CD which are shown in Table 3. Chemical shift changes were calculated from the inclusion complex with respect to both β-CD as well as DL-AGT as $\Delta\sigma = (\sigma_{complex} - \sigma_{DL\text{-}AGT/\beta\text{-}CD})$. In case of β-CD, the upfield shift is more for H3 **(-0.04** ppm) than for H5 (-**0.02** ppm). The result indicates that the inclusion occurred through the wider rim and as the H3 proton shifted to more upfield than the H5 proton .The signals relating to the aromatic protons (**H6', H7'**) of AGT almost remains constant in the spectrum of inclusion complex. However, all the protons related to the piperidine-2,6-dione moiety (**H2', H3', H4' H5')** are upfield shifted as shown in the table 3. Therefore, it can be concluded that only the non-aromatic part were incorporated in the cavity of β-CD after complexation.

It is also evident from the MD studies that the aromatic part of DL-AGT gets stabilised at the narrower end of the beta CD cavity. May be this is the reason of non-shifting of the aromatic protons of DL-AGT.

3.6.2 2D-ROESY NMR Study:

Two-dimensional (2D) NMR spectroscopy provides important information about the spatial arrangement between host and guest atoms by observation of intermolecular dipolar cross-correlations. If two protons are closely located in space i.e., closer than 0.4 nm can produce a nuclear Overhauser effect (NOE) cross-correlation in two-dimensional rotating frame nuclear Overhauser enhancement correlation (2D-ROESY) spectroscopy and therefore Cross-peaks in ROESY spectra will be obtained. The ROESY spectrum of the DL-AGT. β-CD complex (Figure 5b) showed appreciable correlations of H-3' and H-5' protons of DL-AGT with H-3 and H-5 protons of β-CD. These results indicate that the piperidine-2,6-dione moiety of DL-AGT are in close proximity with the H-3 protons of β-CD.These results further confirmed that the DL-AGT.β-CD inclusion complex was successfully formed in the solution phase.

3.7. Molecular Docking study: Molecular docking gives us an effective information about bond simulation between molecules[29].

In order to comprehend the orientation, conformation and interaction of drug/guest molecule within the cavity of β-CD, molecular modelling is a constructive computational technique[30].

Here, docking has been used to predict the possible bound conformation of β-CD.DL-AGT inclusion complex and to estimate the binding affinity[29]. The drug, within the binding cavity of β-CD was docked and the most probable binding conformation was obtained[6]. Results showed that the interaction between DL-AGT and β-CD is 1:1. The drug fitted comfortably within the pocket as shown in the Figure6. The binding affinity for DL-AGT and β-CD was found to be -23.012KJ/mol, which is in good agreement with the experimental findings from UV-Vis spectroscopy. The results also indicated that in the complex only the piperidine-2,6-dione moiety of AGT interacted with the H-3 protons of

CD cavity. The findings of this theoretical study are consistent with the results of FTIR, and NMR experiments.

3.8. SEM study: Scanning Electron Microscopy is one of the best techniques in describing the surface morphology of different chemical entities in solid state. The surface morphologies of host, guest and their inclusion complex have been shown in Figure7. Although both DL-AGT and β-CD are found in crystal form in different sizes. However, DL-AGT appears as irregular-shaped crystal particles with large dimensions(Figure 7A) whereas β-CD appeared as polyhedral crystal like structure(Figure 7B).When, complexation occurs, it is evident that the DL-AGT.β-CD IC (Figure 7C) exhibited a different surface morphology a thread like structure. This distinct surface morphology may be due to the formation of the inclusion complex[23]. The totally dissimilar surface morphology of the inclusion complex may assist the other experimental observations.

3.9. In vitro cell viability study: The synthesized inclusion complex of the drug DL-AGT and β-CD and the drug itself were evaluated for the cell viability study. The cells were exposed to varying concentrations of the drug and inclusion complex and the results of the cell viability obtained in the study have been depicted graphically Fig 8. After the drug treatment, the cell viability was found to be concentration dependent. In case of the drug, as concentration increases, the cell viability of normal kidney cells decreases. But, the cells are more viable in presence of the inclusion complex when compared with the drug. This might be because of the higher toxicity of the drug (DL-AGT) at higher concentration (as the amount of drug increases), normal cells lose their reproducibility and eventually die. But when compared with the inclusion complex the cell viability is more than the original drug as we move lower to higher concentration. So, it is worth mentioning that the complex is less toxic in nature than the drug itself and so the cells are able to grow and reproduce properly. This finding clearly indicates the fact that the inclusion complex is less toxic as it causes less anti-proliferative activity of cell when compared to the drug. This behaviour of the inclusion complex might be due to the controlled release of the drug from the cavity of β-CD[14].

4. Conclusion: In our present study we have synthesized an attainable inclusion complex of an aromatase inhibitory drug DL-AGT and a host β-CD. The process of inclusion was confirmed by ^{1}HNMR, PXRD, FTIR, SEM and the UV-Vis study. From the Job's plot(UV-Visible study) and from the shifting of the H3 and H5 protons of β-CD in the ^{1}HNMR spectra of the IC, it is confirmed that the inclusion occurred in a 1:1 stoichiometric ratio. Moreover, the solubility of the IC in ethanol is greater than the pure drug was also determined. The above experimental observations were further affirmed by molecular docking study, which helps to predict the most stable conformation of the inclusion complex. Lastly the cell viability study between the drug and its IC with β-CD implies that by increasing concentration, the inclusion complex shows less toxicity than the drug itself. So, this is an important finding about the inclusion complex of the drug with β-CD, which may improve the therapeutic activity of the drug towards its application it is meant for and also can change the path of science to a new direction.

Declaration of Competing Interest: No conflict of interest is there.

Acknowledgement: Authors express their gratitude to UGC-SAP, Department of Chemistry, University of North Bengal. Authors are highly indebted to the Department of Biotechnology, University of North Bengal for the Cell viability study.

TABLES

Table 1. Association constants (Ka), Gibb's free energy (ΔG^0), enthalpy (ΔH^0) and entropy (ΔS^0) of AGT-β-CD systems from UV-Vis spectroscopy

Complex	$k_a(10^3M^{-1})$			ΔG^0KJ mol^{-1})	ΔH^0 ($kJmol^{-1}$)	ΔS^0 $Jmol^{-1}$) K^{-1}
	293.15K	303.15K	313.15k			
DL-AGT.β-CI	3.55	2.54	1.59	-19.81	-30.59	-36.16

Table 2:2Θ values of β-CD, DL-AGT and DL-AGT.β-CD inclusion complex from PXRD study.

Components	2Θ
β-CD	4.63, 9.11 , 12.63
DL-AGT	12.38 , 15.09 ,16.75 ,17.95 ,24.92
DL-AGT.β-CD IC	17.85 ,18.50

Table 3: Chemical shifts and its deviations for the protons of β-CD, DL-AGT in free state and in inclusion complex

	Chemical shift σ(ppm)			
Protons	**β-CD**	**DL-AGT**	**DL-AGT.β-CD**	**Δσ ($\sigma_{complex}$-σ_{free})**
H3	3.70		3.66	-0.04
H5	3.58		3.56	-0.02
H2’		5.11	5.07	-0.04
H3’		2.08	2.05	-0.03
H4’		1.81	1.78	-0.03
H5’		0.75	0.73	-0.02
H6’		6.93	6.93	0.0
H7’		6.55	6.55	0.0
Ar-NH_2		10.73	10.73	0.0

*Negative values of Δσ indicate upfield shifts.

Table 4: Binding Affinity of DL-AGT and β-CD from molecular docking

Ligand with receptor	Binding affinity (ΔG^0 KJ/mol)
DL-AGT-β-CD [IC]	-23.012

Table S1: Job plot data of DL-AGT/β-CD system by UV-Visible spectroscopy (at 298.15K).

drug conc. [DL-AGT] (μM)	[β-CD] (μM)	[DL-AGT]/ ([DL-AGT]+ [β-CD])	Absorbance(A) @λ_{max} 238nm	ΔA (0.471953-A)	ΔAx[DL-AGT]/ ([DL-AGT]+[β-CD])
0	100	0	0	0.471953	0
10	90	0.1	0.022884	0.449069	0.044906911
20	80	0.2	0.046735	0.425218	0.085043638
30	70	0.3	0.08291	0.389043	0.116712882
40	60	0.4	0.136551	0.335402	0.134160648
50	50	0.5	0.192047	0.279906	0.139953044
60	40	0.6	0.252155	0.219798	0.13187864
70	30	0.7	0.301264	0.170689	0.119482332
80	20	0.8	0.36616	0.105793	0.08463407
90	10	0.9	0.425218	0.046735	0.042061406
100	0	1	0.471953	8.5E-08	8.5E-08

Table S2: Data of Benesi-Hildebrand double reciprocal plot for DL-AGT.β-CD system from UV-Visible spectroscopy at 293.15K.

A0	A1	ΔA	[β-CD]	1/[β-CD]	1/ΔA
0.350255	0.466103	0.115848	2.0E-05	50000	8.632015
0.350255	0.533593	0.183338	3.0E-05	33333	5.454396
0.350255	0.581200	0.230945	4.0E-05	25000	4.33004
0.350255	0.631231	0.280976	5.0E-05	20000	3.559025
0.350255	0.654953	0.304698	6.0E-05	16667	3.281938
0.350255	0.676511	0.326256	7.0E-05	14286	3.065082

Table S3: Data of Benesi-Hildebrand double reciprocal plot for DL-AGT.β-CD system from UV-Visible spectroscopy at 303.15K.

A0	A1	ΔA	[β-CD]	1/[β-CD]	1/ΔA
0.338275	0.449632	0.111357	2.0E-05	50000	8.980157
0.338275	0.513881	0.175606	3.0E-05	33333	5.694566
0.338275	0.567746	0.229471	4.0E-05	25000	4.357849
0.338275	0.603692	0.265417	5.0E-05	20000	3.767657
0.338275	0.643238	0.304963	6.0E-05	16667	3.27909
0.338275	0.668577	0.330302	7.0E-05	14286	3.027536

Table S4: Data of Benesi-Hildebrand double reciprocal plot for DL-AGT.β-CD system from UV-Visible spectroscopy at 313.15K

A0	A1	ΔA	[β-CD]	1/[β-CD]	1/ΔA
0.317453	0.402578	0.085125	2.0E-05	50000	11.74739
0.317453	0.441405	0.123952	3.0E-05	33333	8.067627
0.317453	0.474593	0.15714	4.0E-05	25000	6.363754
0.317453	0.514473	0.19702	5.0E-05	20000	5.075614
0.317453	0.571728	0.254275	6.0E-05	16667	3.932754
0.317453	0.595930	0.278477	7.0E-05	14286	3.590957

Table S5: Solubility of DL-AGT and DL-AGT.β-CD in ethanol at 25°C.

Sample	Solubility in ethanol ($mg.ml^{-1}$)
DL-AGT	7
DL-AGT.β-CD	17.62

FIGURES

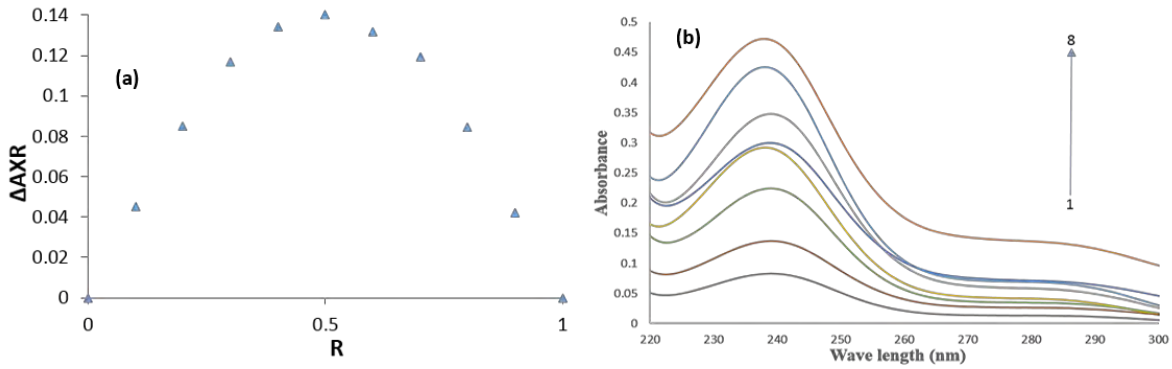

Figure 1: (a) Job plot for the stoichiometry 1:1 (Host:Guest) and (b) Spectra of Job's plot.

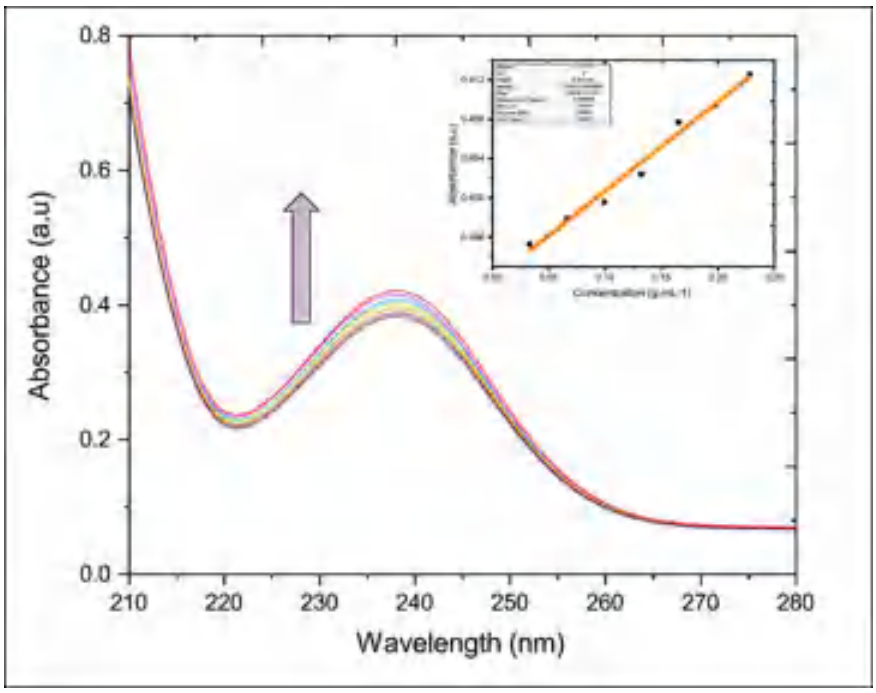

Figure 2: (A) UV spectra of DL-AGT.β-CD with different concentrations ($g.L^{-1}$) in ethanolic solution (at 298.15 K): (a) 0.033; (b) 0.066; (c) 0.099; (d) 0.132; (e) 0.165; (f) 0.198; (g) 0.228. (B) A plot of absorbance ratio of DL-AGT.β-CD at 238 nm vs. the concentration of DL-AGT.β-CD (inside the box)

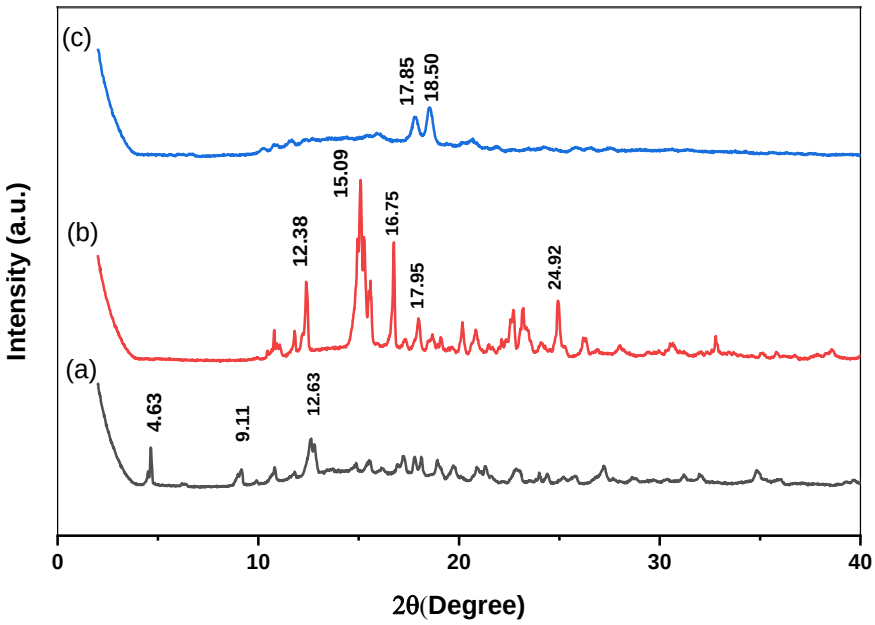

Figure 3: PXRD diffractogram of (a) β-CD, (b) DL-AGT and (c) DL-AGT.β-CD IC (inclusion complex)

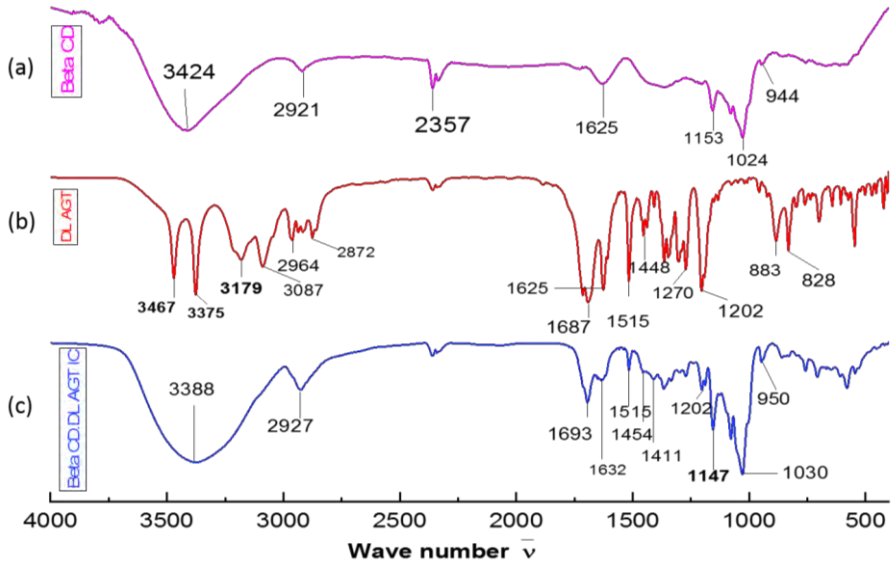

Figure 4: Infrared spectra of (a) β-CD, (b) DL-AGT and (c) β-CD.DL-AGT IC (Inclusion complex)

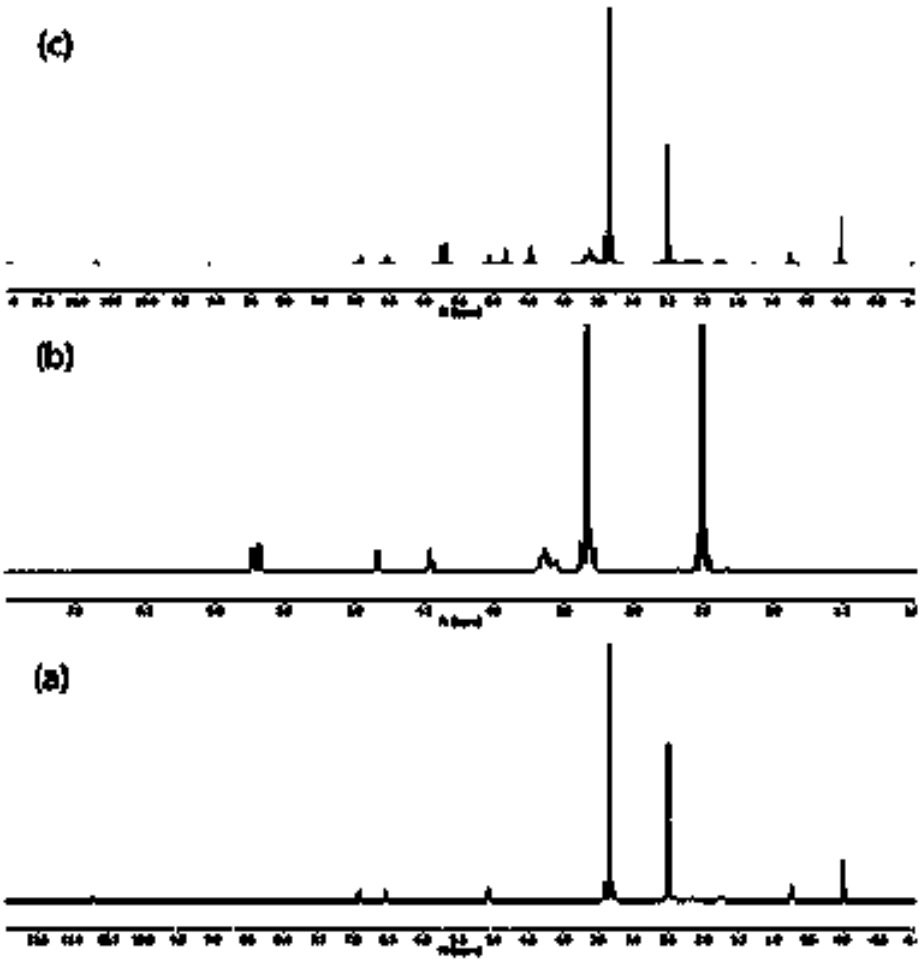

Figure 5a: ^{1}H NMR spectra of (a) DL-AGT (b) β-CD and (c) β-CD.DL-AGT IC

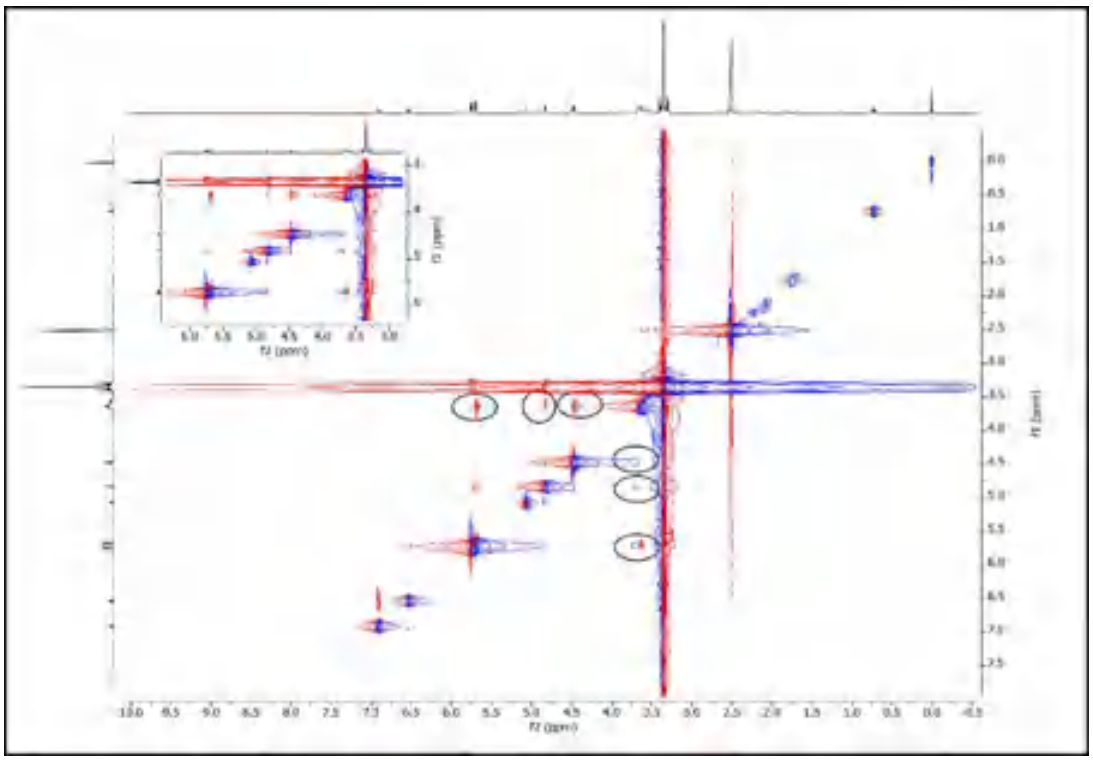

Figure 5b: ROESY spectrum of β-CD.DL-AGT IC in D_6-DMSO

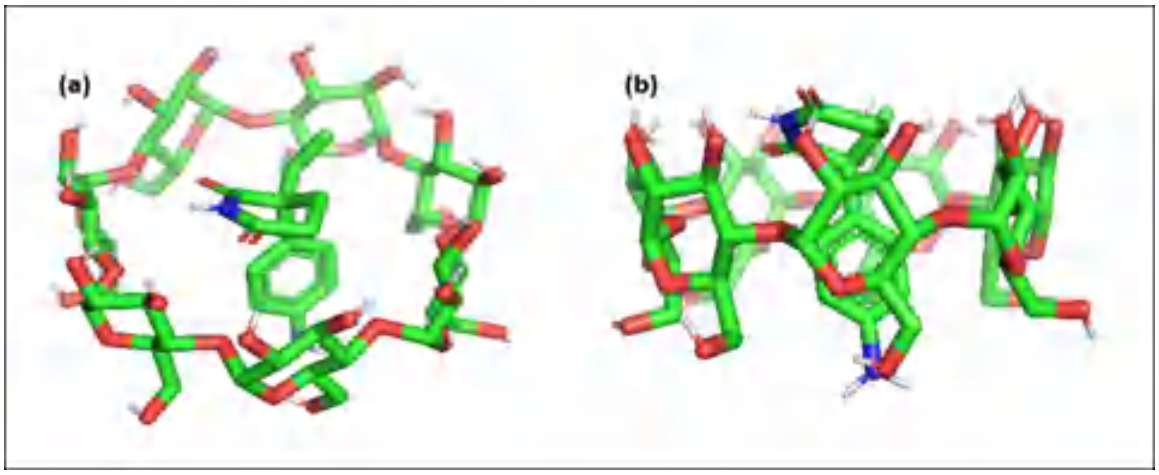

Figure.6: Mode of binding of the drug DL-AGT into β-CD [IC] (a) Top view (b) Side view

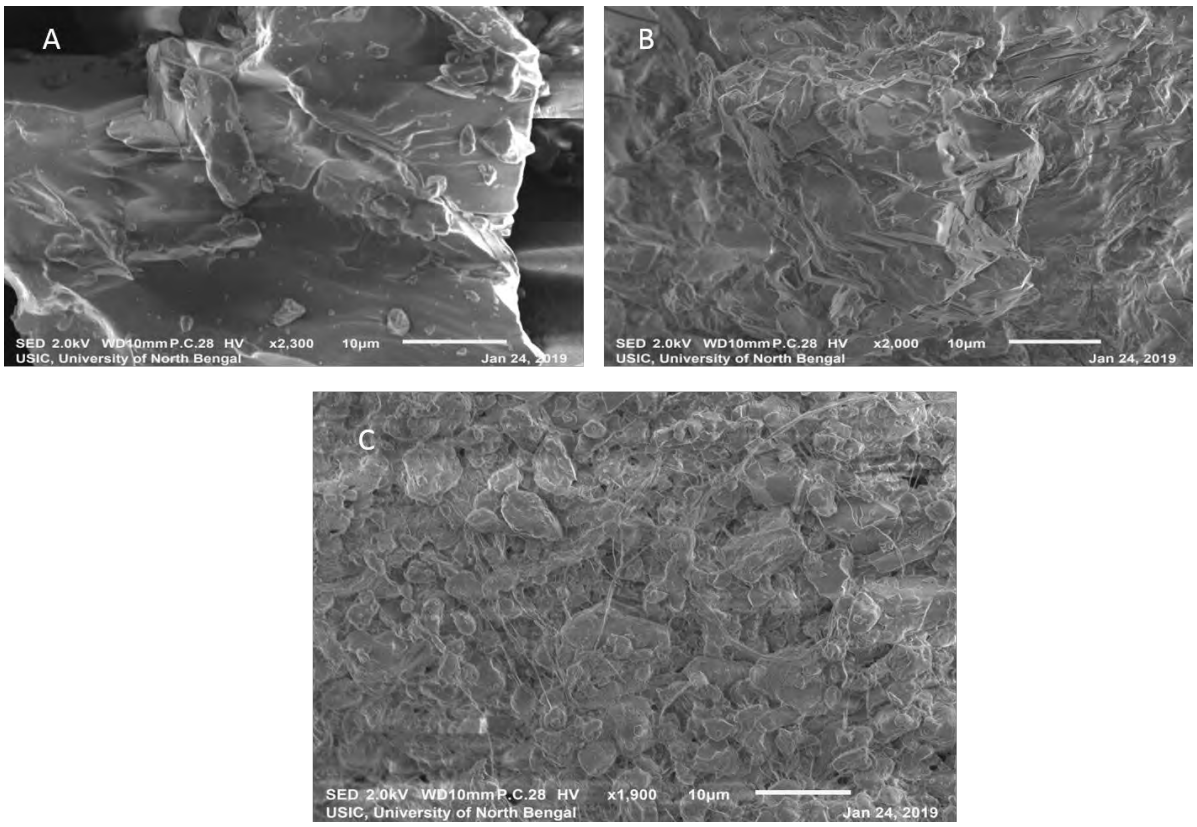

Figure7: SEM images of (A) DL-AGT (B) β-CD and (C) β-CD.DL-AGT IC.

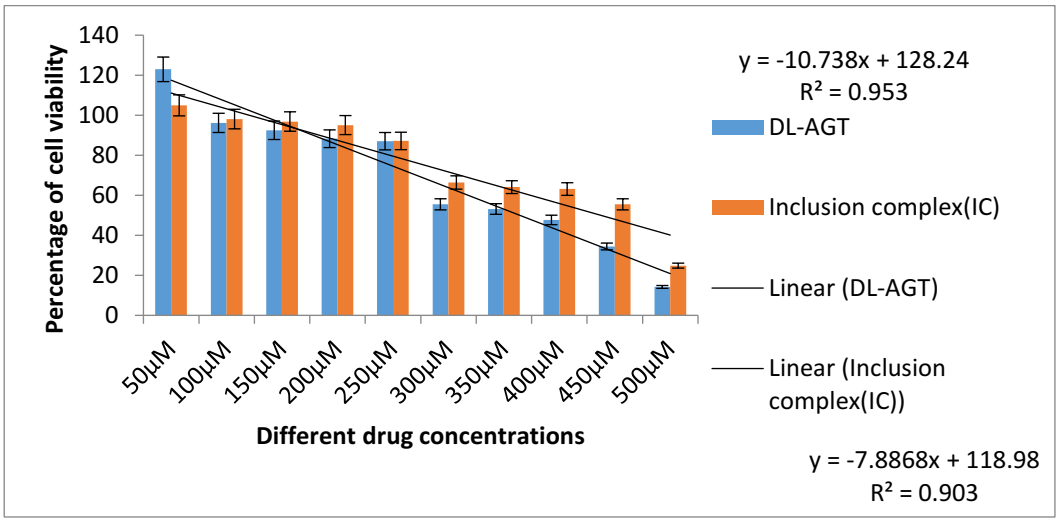

Figure8: In-vitro cell viability study of pure drug and its Inclusion complex

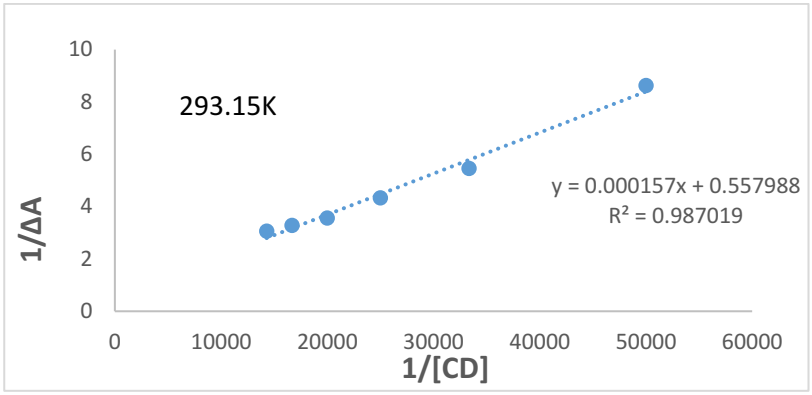

Figure S1: Benesi-Hildebrand double reciprocal plot at temperature 293.15K

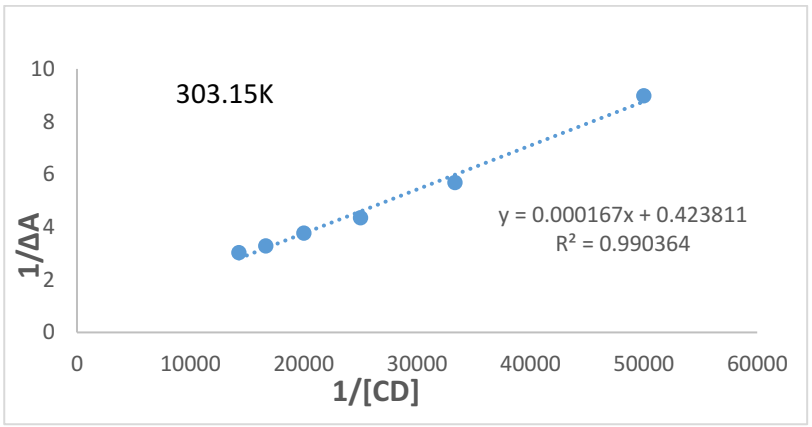

Figure S2: Benesi-Hildebrand double reciprocal plot at temperature 303.15K

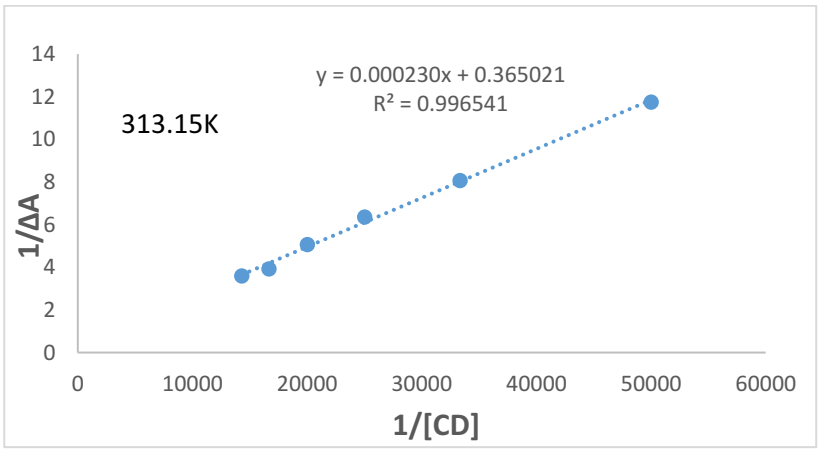

Figure S3: Benesi-Hildebrand double reciprocal plot at temperature 313.15K

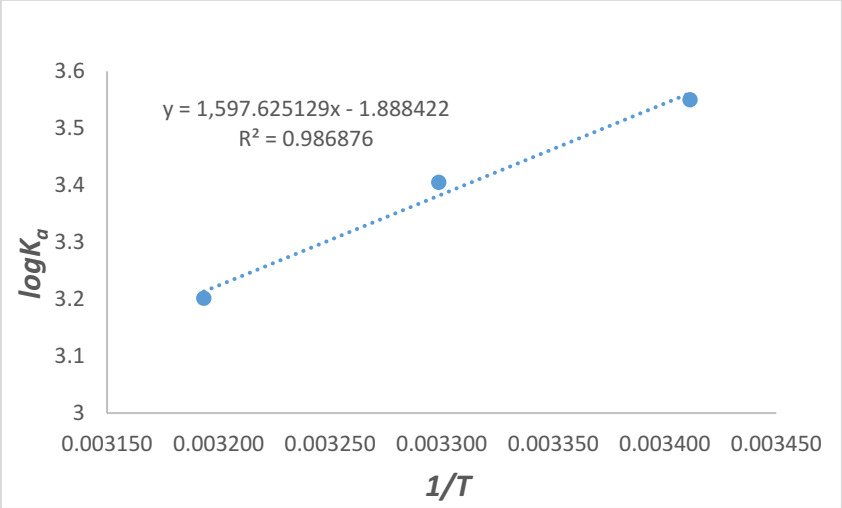

Figure S4: Plot of $logk_a$ Vs 1/T (from where the thermodynamic parameters were determined)

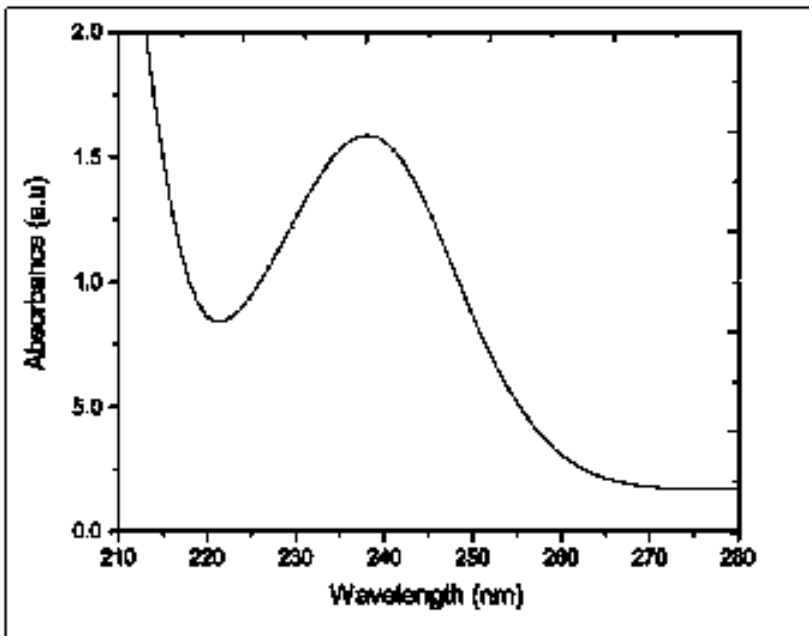

Figure S5: Absorption spectra of DL-AGT.β- CD inclusion complex with saturated concentration in ethanolic solution.

SCHEMES

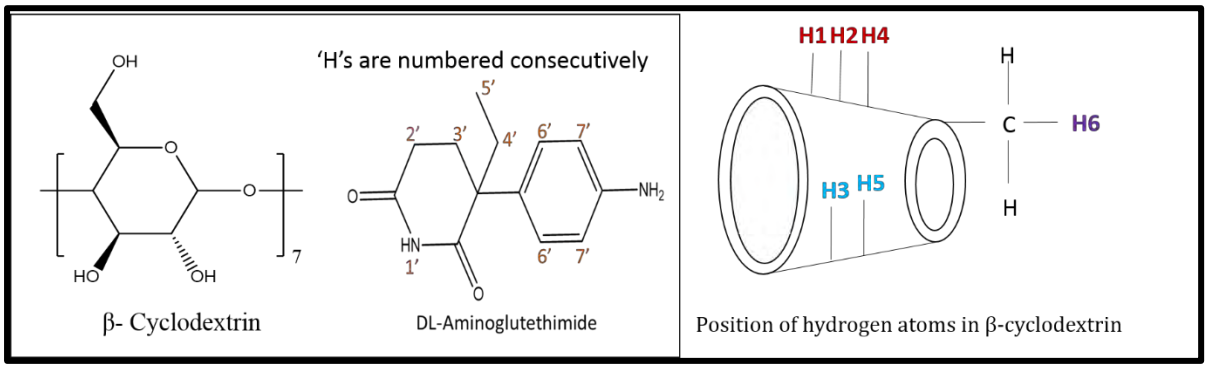

Scheme.1: Structures of the concerned molecules.

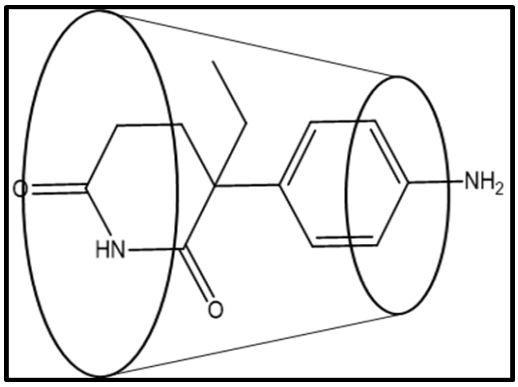

Scheme.2: The plausible mechanism of inclusion.